Novel Electrodes for Underwater ECG Monitoring

Bersain A. Reyes, *Student Member, IEEE*, Hugo F. Posada-Quintero, *Student Member, IEEE*, Justin R. Bales, Amanda L. Clement, George D. Pins, Albert Swiston, Jarno Riistama, John P. Florian, Barbara Shykoff, Michael Qin, and Ki H. Chon*, *Senior Member, IEEE*

***Abstract*—We have developed hydrophobic electrodes that provide all morphological waveforms without distortion of an ECG signal for both dry and water-immersed conditions. Our electrode is comprised of a mixture of carbon black powder (CB) and polydimethylsiloxane (PDMS). For feasibility testing of the CB/PDMS electrodes, various tests were performed. One of the tests included evaluation of the electrode-to-skin contact impedance for different diameters, thicknesses, and different pressure levels. As expected, the larger the diameter of the electrodes, the lower the impedance and the difference between the large sized CB/PDMS and the similarly-sized Ag/AgCl hydrogel electrodes was at most 200 kΩ, in favor of the latter. Performance comparison of CB/PDMS electrodes to Ag/AgCl hydrogel electrodes was carried out in three different scenarios: a dry surface, water immersion, and postwater immersion conditions. In the dry condition, no statistical differences were found for both the temporal and spectral indices of the heart rate variability analysis between the CB/PDMS and Ag/AgCl hydrogel ($p > 0.05$) electrodes. During water immersion, there was significant ECG amplitude reduction with CB/PDMS electrodes when compared to wet Ag/AgCl electrodes kept dry by their waterproof adhesive tape, but the reduction was not severe enough to obscure the readability of the recordings, and all morphological waveforms of the ECG signal were discernible even when motion artifacts were introduced. When water did not penetrate tape-wrapped Ag/AgCl electrodes, high fidelity ECG signals were observed. However, when water penetrated the Ag/AgCl electrodes, the signal quality degraded to the point where ECG morphological waveforms were not discernible.**

***Index Terms*—Carbon black-PDMS, ECG electrode, ECG monitoring, heart rate variability (HRV), reusable, underwater, waterproof.**

I. Introduction

THE heart rate (HR) derived from an electrocardiogram (ECG) measurement is widely used and accepted as one of the key vital signs [1]. Certainly, much important physiological information can be deduced from both HRs and morphological changes in the ECG waveforms. In nonwater immersed conditions, the benefits of ECG recordings for assessing cardiovascular and physiological health have been well documented. We surmise that similar invaluable information can be garnered when a subject is fully immersed in water but the evidence is scant since ECG electrodes that can operate in water-submersed environments at hyperbaric depths for prolonged periods have not yet been developed.

The significant hyperbaric pressure and cold temperatures associated with increasing depth underwater are known to cause severe challenges to the human physiological control systems [2]. When the control systems break down due to prolonged hyperbaric exposures, humans are more susceptible to detrimental conditions such as hypothermia, hypoxia, and many neurological and cardiovascular problems including decompression sickness (DCS) [3]–[7]. For the aforementioned hazardous conditions, early detection is crucial for taking prompt corrective actions. Beyond the HR, information derived from morphological changes in the ECG waveform can be used to diagnose cardiac ischemia, injury, and malignant arrhythmias [8], [9]. Recently, our research group has shown that early detection of DCS can be made from HR variability (HRV) analysis [6]. Specifically, it was found that for neurological DCS, which is the most severe form of DCS, there was significant depression of the sympathetic and parasympathetic tones as determined by the HRV analysis [6]. For cardiopulmonary DCS, we found elevated parasympathetic but reduced sympathetic tone [10]. Hence, a diving monitor that can measure ECG signals so that HRV analysis can be performed is needed if early detection of DCS and the proper counter measures can be developed to prevent injuries due to prolonged exposure to a hyperbaric environment.

A fully functional and reliable underwater ECG monitoring system, capable of recording ECG waveforms even with water infiltration, does not currently exist to support either shallow or deep diving medical research. Recently, a device that has potential for long-term ECG monitoring has been trialed, but it relies on using Ag/AgCl electrodes that are held in place with

Manuscript received October 3, 2013; revised January 9, 2014 and February 24, 2014; accepted February 27, 2014. Date of publication March 6, 2014; date of current version May 15, 2014. This work was supported by the Office of Naval Research work unit N00014-12-1-0171. The Lincoln Laboratory portion of this work was sponsored by the Assistant Secretary of Defense for Research & Engineering under Air Force Contract FA8721-05-C-0002. Opinions, interpretations, conclusions and recommendations are those of the authors and are not necessarily endorsed by the United States Government. *Asterisk indicates corresponding author.*

B. A. Reyes, H. F. Posada-Quintero, J. R. Bales, and A. L. Clement, and G. D. Pins are with the Department of Biomedical Engineering, Worcester Polytechnic Institute, Worcester, MA 01609 USA (e-mail: bareyes@wpi.edu; hposadaquintero@wpi.edu; justin.r.bales@wpi.edu; ablackwood@wpi.edu; gpins@wpi.edu).

A. Swiston is with MIT Lincoln Laboratory, Lexington, MA 02421 USA (e-mail: albert.swiston@ll.mit.edu).

J. Riistama is with Philips Research, 5656 AE Eindhoven, The Netherlands (e-mail: jarno.riistama@philips.com).

J. P. Florian and B. Shykoff are with the Navy Experimental Diving Unit, Panama City, FL 32407 USA (e-mail: john.florian@navy.mil; barbara.shykoff.ca@navy.mil).

M. Qin is with the Naval Submarine Medical Research Laboratory, New London, CT 06349 USA (e-mail: Michael.Qin@med.navy.mil).

*K. H. Chon is with the Department of Biomedical Engineering, Worcester Polytechnic Institute, Worcester, MA 01609 USA (e-mail: kichon@wpi.edu).

Color versions of one or more of the figures in this paper are available online at http://ieeexplore.ieee.org.

Digital Object Identifier 10.1109/TBME.2014.2309293

water-resistant tape [11], [12]. Good adhesion to skin after adequate skin preparation makes the standard wet Ag/AgCl electrodes the universal option for clinical and research application [13]. However, some limitations of the wet Ag/AgCl electrodes include skin irritation, bacterial growth especially for long-term recordings, gel dehydration over time, and signal degradation with sweat [14]. In addition, unopened Ag/AgCl electrode packages have expiration dates that complicate inventory management. Both their obsolescence and disposability increases costs. For these and other reasons, it is difficult to incorporate Ag/AgCl electrodes into a neoprene protective wetsuit, especially because the electrodes' functioning falters in underwater condition. A moleskin tape, which is taped over a waterproof tape, is often used to further preclude water penetration [15]. However, the consequence is severe skin irritation due to the tape and peeling off the moleskin can often lead to tearing of the skin. Donning a dry suit is an option to prevent water penetration but it is expensive compared to a wet suit and it is limited to cold water applications.

Dry electrodes have been considered as an alternative to replace conventional wet Ag/AgCl electrodes for long-term ECG recordings, particularly because they do not require an electrolyte layer [16]–[18]. Recently, use of carbon nanotube-Polydimethylsiloxane (PDMS) based dry electrodes was proposed for ECG and electroencephalographic (EEG) recordings [14], [19]. In particular, ECG carbon nanotube/PDMS dry electrodes exhibited superior performance to other dry electrodes and were found to be robust even when subjects perspired [14]. However, the fabrication process is expensive and complicated. In addition, no studies were conducted to analyze the performance of these carbon nanotube-based electrodes during full water immersion.

Given the lack of electrodes that are fully functional in water immersion without the use of waterproof adhesive tape, we will illustrate in this paper the development of a novel carbon black powder/PDMS (CB/PDMS) composite electrode for ECG monitoring. In this paper, we describe 1) the fabrication process of the electrodes, 2) determination of the optimal size of the electrodes with respect to their impedance values, 3) cytotoxicity tests, and 4) evaluation of CB/PDMS electrodes for ECG data collection during both dry and full water immersion conditions. All experiments and data analyses to determine ECG signal fidelity compare the CB/PDMS electrodes to the Ag/AgCl electrodes as the latter are the standard in practice.

II. Materials and Methods

A. Fabrication of CB/PDMS Electrodes

Electrodes were fabricated of a conductive element comprising CB and PDMS based on previous studies [20], [21]. Electrodes were fabricated using the following steps:

1) Conductive CB powder (CB Super P Conductive, Alfa Aesar; Ward Hill, MA, USA) is used as the conductive material. PDMS (Sylgard 184, Dow Corning; Auburn, MI, USA) was used as the insulating matrix.
2) The CB/PDMS mixture was then mixed with the PDMS curing agent according to a previous study and manufacturing recommendations [22].
3) The CB/PDMS/curing agent mixture was poured and leveled with a straight metal edge into wells of the electrode molds, forming disks.
4) The mixture was applied to the reverse side of nickel plated snap fasteners appropriately sized for conventional ECG monitor connection.
5) All components were degassed in a vacuum chamber to remove air bubbles.
6) The fasteners were affixed to the molded CB/PDMS/curing agent mixture with gentle pressure without causing major rippling.
7) The filled mold assembly was then placed in a curing oven.
8) The molds were disassembled and the electrodes removed.

TABLE I
Dimensions of the CB/PDMS Electrodes Fabricated

Carbon Black/PDMS electrode	Diameter (cm)	Thickness (mm)
Small-thin	2	2
Small-thick	2	3
Large	3	2

Plates containing circular molds of different sizes were designed using Inventor 3D CAD software (Autodesk Inc.; San Rafael, CA, USA) and 3-D printed in Acrylonitrile–Butadiene–Styrene plastic. Mold sizes were designed to produce CB/PDMS electrodes of three different dimensions (diameter and thickness) as shown in Table I.

A total of 14 electrodes of each size were produced for impedance characterization and ECG data collection. To observe the topographical information of the CB/PDMS electrodes, scanning electron microscope (SEM) images were obtained in high vacuum at different magnifications.

B. Impedance Characterization

The electrode-skin contact impedance was analyzed for the three different sizes of CB/PDMS electrodes. For each electrode size, seven pairs of electrodes were selected. The impedance was measured using an impedance analyzer (IM3570, Hioki E.E. Corporation; Cranbury, NJ, USA) by averaging 20 measurements at each of 25 logarithmically equally-spaced frequencies ranging from 4 to 100 kHz. For each measurement, two CB/PDMS electrodes of the same dimensions were placed on anterior forearm skin 2 cm apart from each other. While ECG power is mostly below 40 Hz, selection of the measurement frequency range to 100 kHz and the location of the electrodes for impedance measurements were chosen so that our results can be compared to previous other studies [14], [16]. An elastic compression bandage was used to fix them to the skin. Prior to each measurement, the skin area was cleaned with 70% isopropyl alcohol but shaving or scrubbing of the surface area was not done. Three different pressure levels were applied to the electrodes to fix them to the skin: 1) low pressure level, 2) medium pressure level, and 3) high pressure level; the low pressure was defined as

the minimal contact force needed to adhere the electrodes to the skin, and the high pressure as the maximal force comfortable for the subject. To allow all electrodes an equal time to stabilize on the skin surface, measurements were started 30 s after fixation. All measurements were performed on the same day to keep skin properties as constant as possible [16]. Finally, baseline impedance of the measurement device itself was measured and it was found to have a maximum value of 315 mΩ.

C. Cytotoxicity Test

Cell Culture: Direct contact cytotoxicity assays were performed on confluent monolayers of L929 mouse connective tissue fibroblasts (CCL-1; ATCC, Manassas, VA, USA) or pooled neonatal normal human epidermal keratinocytes (NHEK; Lonza, Walkersville, MD, USA). L929 cells were cultured in high glucose Dulbecco's Modified Eagle Medium (DMEM; Life Technologies, Carlsbad, CA, USA) supplemented with 10% characterized fetal bovine serum (FBS; Hyclone, Logan, UT, USA) and 100 U-mL/100 mg-mL/2 mM penicillin/streptomycin/L-glutamine (Life Technologies, Carlsbad, CA, USA). Cultures were maintained in a 37 °C incubator at 5% CO_2 and passaged according to ATCC recommendations at 80%–90% confluence. For cytotoxicity experiments, L929 cells were seeded at a density of 27 000 cells/cm^2 in six well plates and grown to confluence. NHEKs were cultured in KGM-Gold medium (NHEK; Lonza, Walkersville, MD, USA) at 37 °C and 5% CO_2. NHEKs were subcultured according to Lonza recommendations between 80%–90% confluence. For cytotoxicity experiments, NHEKs were seeded at a density of 10 000 cells/cm^2 in six well plates and grown to confluence. Experiments were performed on NHEKs between passages two and four.

Direct Contact Cytotoxicity Assay: To assess the cytotoxicity of the electrodes, direct contact cell culture evaluation was carried out per ASTM F813-07. Small-thin CB/PDMS electrodes (2-cm diameter × 2-mm thickness), positive control latex disks (19 mm diameter × 1.6 mm; McMaster-Carr, Princeton, NJ, USA), and negative control high density polyethylene disks (HDPE; 19 mm in diameter × 2.4 mm in; McMaster-Carr, Princeton, NJ, USA) were sterilized by overnight incubation in an antibiotic cocktail containing 100 U/mL-100 μg/ml penicillin-streptomycin, 2.5 μg/mL amphotericin B, 10 pg/mL ciproflaxin, and 100 μg/mL gentamycin. Alternatively, electrodes were sterilized by autoclaving. Antibiotic sterilized samples were rinsed in three washes of culture medium prior to testing. Culture medium was aspirated, material samples were placed in the center of the confluent cell monolayers, and fresh medium was added. Additional HDPE was used to weigh down electrodes and latex to minimize sample movement, as per ASTM F813-07. Cells were incubated with material for 24 h, and the morphology of cells was assessed by phase contrast microscopy. Wells with no cells and no added material were used as background controls.

MTT Assay: Cell viability was assessed using an MTT reduction assay to measure cell metabolic activity. Samples were removed from wells and cultures were rinsed once with Versene solution (Lonza, Walkersville, MD, USA) to remove nonadherent cells. Cultures were incubated in medium supplemented with 1 mg/mL 3-(4, 5-dimethylthiazol-2-yl)-2, 5-diphenyl tetrazolium bromide (MTT; Sigma, St. Louis, MO, USA). After 2 h at 37 °C, unreacted MTT was aspirated and wells were imaged. The formazan product was solubilized with 1 mL dimethyl sulfoxide (DMSO) per well and the supernatant was diluted 1:4 with DMSO. The optical density (OD) was measured in duplicate in a microplate (100 μl/well) at 540 nm using a SpectraMax 250 plate reader. Data for each sample was normalized between experiments using the following equation:

$$\%\text{Cellular activity} = \frac{\text{OD}_{\text{sample}} - \text{OD}_{\text{no cells}}}{\text{OD}_{\text{no material}}} \times 100 \quad (1)$$

where $\text{OD}_{\text{no cells}}$ is the average OD reading of MTT incubated in wells containing no cells and $\text{OD}_{\text{no material}}$ is the average OD reading of MTT incubated in wells containing cells but no added sample material.

Statistical Analysis: Cytotoxicity experiments were conducted three times with samples in triplicate. Statistical differences for cytotoxicity studies were evaluated using SigmaPlot Version 11.0 (Systat Software, Inc.). One Way Analysis of Variance (ANOVA) with Holm–Sidak posthoc analysis was performed. Because the NHEK data was heteroscedastic, ANOVA with Holm–Sidak was also performed on base ten logarithmically transformed data to ensure statistical robustness; results were unchanged. A significant difference between groups was indicated by a p value <0.05.

D. ECG Data Collection

Subjects: Twelve healthy male volunteers of ages ranging from 20 to 51 years (mean ± standard deviation 29.50 ± 8.93), weight 74.80 ± 8.93 kg, and height 174.90 ± 5.34 cm, were enrolled in this study. The group consisted of students and staff members from Worcester Polytechnic Institute, MA, USA. The study protocol was approved by the Institutional Review Board of WPI and all volunteers consented to be subjects for the experiment.

Equipment: Three Holter recorders were simultaneously used to acquire ECG signals from volunteers (RZ153+, Rozinn Electronics, Glendale, NY, USA) with three different electrodes as detailed below in the Protocol section. These Holter recorders provide a frequency response between 0.05 to 60 Hz at −3 dB and a sampling frequency of 180 Hz. Acquired signals were saved in CompactFlash Card Readers for subsequent offline data analysis.

Protocol: Simultaneous ECG signals were acquired using conductive adhesive gel electrodes (Cleartrace 1700, CONMED, Utica, NY, USA), small-thin CB/PDMS, and large CB/PDMS. The conductive adhesive gel electrodes used had an active circular area of 2 cm in diameter and will be referred to as wet Ag/AgCl. All sets of electrodes were contiguously placed to create a one-channel ECG recording. Electrodes were placed: on xiphoid process (ground), center of the manubrium (1−), and under the left pectoral near V6 electrode position (1+). This configuration mimics the traditional Lead II ECG [23]. The three

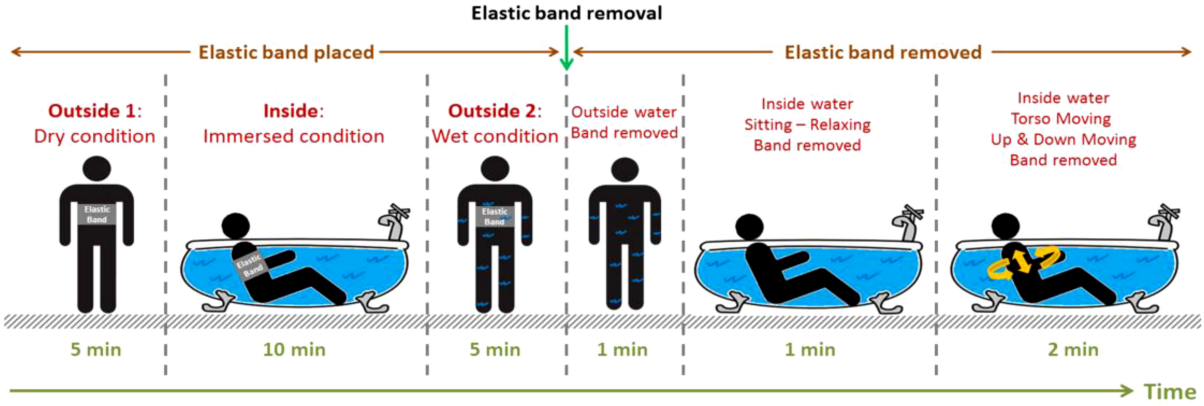

Fig. 1. ECG data acquisition protocol involving dry, immersed, and wet conditions. The elastic band removal was performed for only three subjects.

sets of electrodes were randomly placed on all subjects around the selected locations. Randomization of the Holter recorders was also done. Note that the CB/PDMS electrodes were reused throughout the two weeks of underwater data collection. After cleaning the skin sites with 70% isopropyl alcohol, CB/PDMS electrodes were placed with a regular surgical tape (Transpore, 3M, St. Paul, MN, USA) while wet Ag/AgCl electrodes were directly placed on the skin as their surface is completely adhesive.

To ensure all electrodes were well adhered to the body and minimize the penetration of water to the Ag/AgCl gel, the thoracic area was wrapped with an elastic compression band. A reliable ECG signal from Ag/AgCl electrodes was needed so that the signal from the CB/PDMS electrodes could be compared to it. Once the first three protocols of the experiment were completed (see below), the elastic compression band was removed from all electrodes to determine the full hydrophobicity of both the Ag/AgCl and CB/PDMS electrodes.

Each experiment was of 20 min in duration and was divided into four periods (see Fig. 1) as follows:

1) 5 min in standing position outside the bathtub (dry condition).
2) 10 min in seated position inside the water-filled bathtub (immersed condition).
3) 5 min in standing position outside the bathtub (wet condition).
4) For three subjects, the elastic compression band was removed and an additional 5 min recording was acquired with the subjects standing outside the bathtub (1 min), seated inside the bathtub without any movement (2 min, moving their torsos side-to-side inside the bathtub (1 min), and moving their torsos up-and-down inside the bathtub (1 min).

All recordings were collected at the WPI Sports Center. Bathtub water temperature was controlled (mean $\pm$ standard deviation 33.3 $\pm$ 1.34 °C). This facility is equipped with bathtubs for athletes' training and rehabilitation. During the first period, subjects were asked to remain relaxed in standing position outside the bathtub; the electrodes at this point were completely dry. During the immersed condition, subjects were asked to be seated inside the bathtub with the water coming up to their neck so that all electrodes were fully immersed. Finally, the subjects were asked to exit the bathtub and remain relaxed in standing position with the wet electrodes still applied to their skin. For three subjects, the elastic compression band was removed and the subjects were re-immersed in the water in a sitting position. Data were recorded for 2 min with subjects performing up-and-down and side-to-side movements. The aim for this portion of the experiment was to compare hydrophobicity of the two types of electrodes during body movements in water immersed condition.

Signal processing: Acquired ECG data were first filtered with a 4th order Butterworth filter with a pass-band between 0.05 to 40 Hz and applied in forward and reverse scheme to produce zero-phase distortion and minimize the start and end transients. As recently proposed for ECG signal denoising [24], a second filtering step was applied by using a nonlocal mean filtering algorithm in order to minimize the white Gaussian noise observed in the collected data [25].

After filtering, simultaneous ECG recordings from different Holter monitors were aligned by using the cross-correlation function; 20 s of acquisition were extracted from each recording to compute the cross-correlation sequence and then the sample lag which provides the maximum cross-correlation value was used to align the ECG recordings by shifting the corresponding recording by that amount of samples. Data containing motion and noise artifacts were omitted for further data analysis. For each condition, a segment of at least two consecutive minutes was manually extracted from the simultaneous Holter recordings and then aligned. The data inclusion criterion was that ECG signals from the three Holter recorders all had to contain relatively noise-free measurements. Our choice of requiring data duration of at least 2 min was so that spectral dynamics associated with the HRV analysis could be obtained [8].

R-wave peak detection was performed on all selected ECG segments by using a robust QRS complex detection algorithm [26], [27]. Manual correction of R-wave peak locations was performed when necessary and subsequently RR interval time series were calculated. A sampling frequency of 4 Hz was used on the RR intervals by cubic spline interpolation. The power spectral densities of the interpolated RR time series were computed with Welch's modified periodogram method with 50% overlap, NFFT = 1024 (frequency resolution of 0.0039 Hz)

and a Hamming window was used to compute the power spectral density.

ECG templates were computed for each selected ECG segment by creating an ensemble matrix with the corresponding ECG cycles aligned with respect to their R-peak locations and finally averaged at each time instant.

Performance Evaluation: CB/PDMS electrode performance was tested by extracting temporal and spectral parameters from the RR intervals as defined in the literature [8]. Signals acquired with wet Ag/AgCl electrodes with subjects in dry conditions were used as reference, and for our short-duration experiments, the elastic compression band wrapped over the electrodes provided even stronger adhesive bonding to the skin that water did not penetrate. We used HRV analysis as a quantitative performance measure since most previous hyperbaric studies [4], [6], [10], [28] were concerned with changes in the dynamics of the autonomic nervous system, and our recent work has shown a promising approach for early detection of DCS in swine by tracking changes in the sympathetic and parasympathetic nervous tones via the HRV [6], [10].

Temporal measures of HRV considered in this study were 1) mean RR interval (millisecond units), 2) SDNN (standard deviation of all RR intervals, millisecond units), 3) RMSSD (square root of the mean of the sum of the squares of differences between adjacent RR intervals, millisecond units), and 4) NN50 count (number of pairs of adjacent RR intervals differing by more than 50 ms in the entire recording, unitless).

Spectral measures of HRV from short-term recordings considered were 1) LF (power in low frequency band from 0.04–0.15 Hz, squared millisecond units), 2) HF (power in high frequency band from 0.15–0.4 Hz, squared millisecond units), 3) the total power (squared millisecond units), and 4) HF/LF ratio (unitless).

Peak-to-peak amplitude of ECG templates was used to quantify the amplitude reduction of the ECG signals when electrodes were immersed in water. The cross-correlation coefficient between the ECG templates obtained with CB/PDMS electrodes and with wet Ag/AgCl electrodes was used to quantify the signal distortion as defined by

$$\rho = \frac{\sum_{i=1}^{N} \overline{\mathrm{ECG}}_{\mathrm{Ag/AgCl}} \cdot \overline{\mathrm{ECG}}_{\mathrm{CB/PDMS}}}{\sqrt{\sum_{i=1}^{N} \left(\overline{\mathrm{ECG}}_{\mathrm{Ag/AgCl}}\right)^2 \cdot \sum_{i=1}^{N} \left(\overline{\mathrm{ECG}}_{\mathrm{CB/PDMS}}\right)^2}} \quad (2)$$

where $\overline{\mathrm{ECG}}_x$ represents the ECG template obtained with the corresponding electrodes, and N is the length of the ECG templates. Finally, temporal and spectral measures of HRV, and peak-to-peak amplitude of ECG templates, obtained from recordings with large and small-thin CB/PDMS electrodes were compared with those obtained with wet AG/AgCl electrodes using the paired t-test with $p < 0.05$ considered as significant.

III. Results

A. CB/PDMS Electrodes

Circular ECG electrodes were fabricated by using a CB/PDMS mixture. The dimensions (diameter and thickness) of the electrodes were controlled via 3-D printed molds. Fig. 2 shows an example of each size of fabricated CB/PDMS electrodes. Microstructure of CB/PDMS electrodes was observed via high-vacuum SEM micrographs after freeze-fracture as shown in Fig. 3. Deposition and well-distributed CB particles inside the elastomeric matrix is seen.

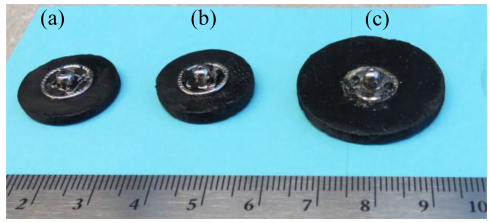

Fig. 2. CB/PDMS electrodes. Left to right: (a) small-thin electrode, (b) small-thick electrode, (c) large electrode. Rules scale in cm.

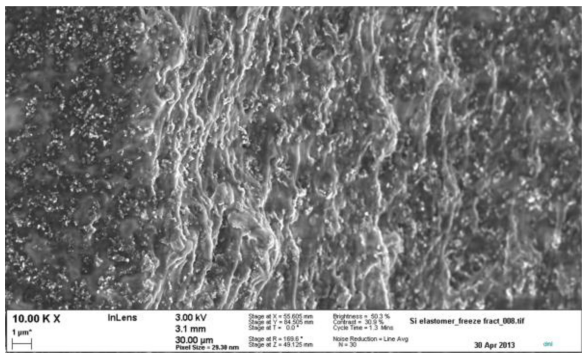

Fig. 3. High-vacuum SEM image of CB/PDMS electrodes. Scale bar = 1000 nm.

B. Impedance Characterization

CB/PDMS electrode-skin contact impedance was measured for the three different dimensions at three pressure levels. For reference, the results are compared to wet Ag/AgCl electrode-skin impedance at the same position; the reported impedance magnitude $|Z|$ values were plotted versus frequency in Fig. 4 and are in agreement with previously-reported studies [16].

For all electrode sizes, the impedance was dependent on the applied pressure and its value decreased with increasing frequency. For all pressure levels, the impedance was lower for the large electrodes (3 cm $\times$ 2 mm) compared to either the thick or thin small electrodes (2 cm diameter); among these small electrodes, the impedance was lower for the thin (2 mm) than for the thick electrodes (3 mm). For the two thinner electrodes (2 mm thickness) there was only a slight difference between medium and high pressure levels. The wet Ag/AgCl electrodes were not affected by the difference in the applied pressure. Measurements of the CB/PDMS electrode-skin impedance obtained at 33 Hz for the different applied pressure levels is shown in Table II. This table summarizes the findings of the electrode-skin impedance results at a representative frequency of the ECG spectrum. For reference, the wet Ag/AgCl electrodes had an electrode-skin impedance around 80 kΩ at 33 Hz. Measurements of CB/PDMS electrode-skin impedance were performed on an additional subject several days after and the results are

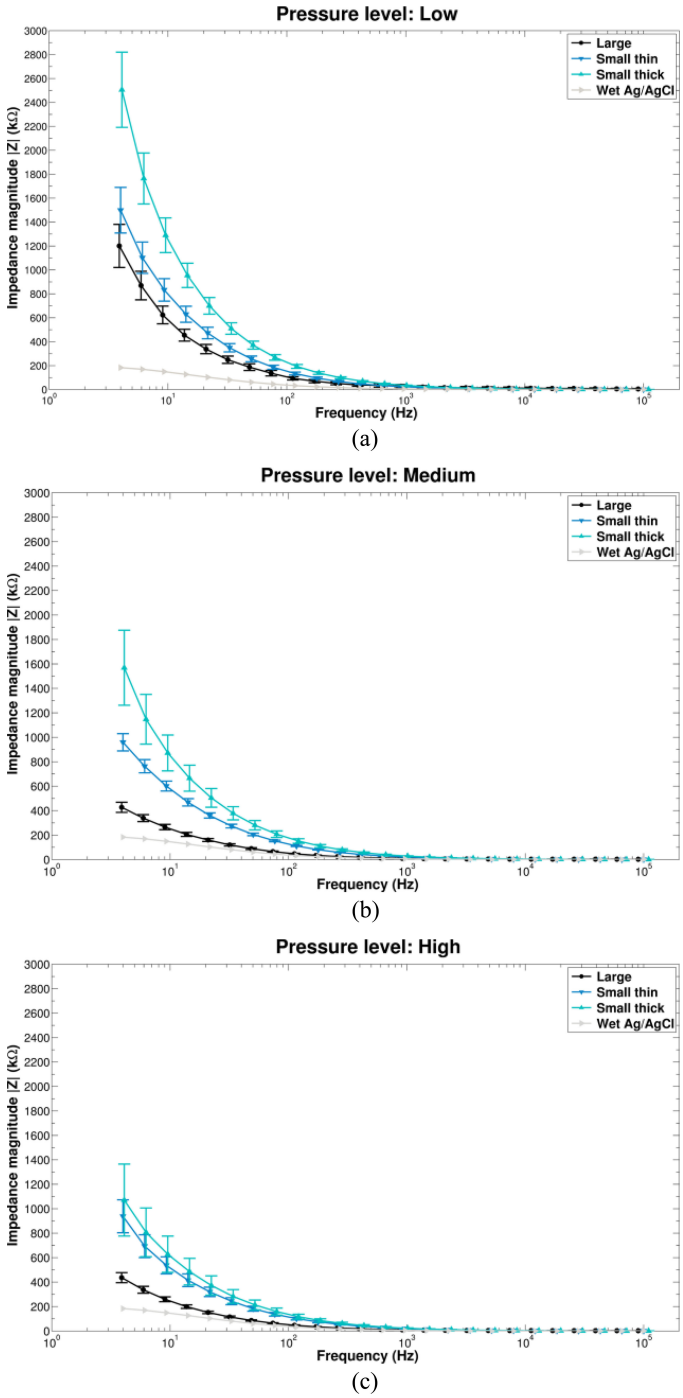

Fig. 4. Impedance of different CB/PDMS electrode sizes at same pressure level. (a) Low pressure. (b) Medium pressure. (c) High pressure.

similar to the findings of Fig. 4. For example, the observations of the pressure dependence of the CB/PDMS-skin impedance and lower impedance of the large electrodes when compared to the small ones remained intact.

Given that large CB/PDMS electrodes with a medium or high pressure level showed lower electrode-skin impedance magnitude followed by the small-thin CB/PDMS electrodes, we used these two configurations for measuring human ECG recordings during dry, water immersion, and wet conditions. For the recording experiments outside and inside the water-filled bathtub, all large and small-thin CB/PDMS electrodes were fixed to the body by applying medium pressure with a stretchable compression band.

TABLE II
ELECTRODE-SKIN IMPEDANCE MEASUREMENTS AT 33 HZ FOR THE CB/PDMS ELECTRODES AT DIFFERENT PRESSURE LEVELS

Electrodes	Low pressure	Medium pressure	High pressure
Small-thick	510 ± 127	378 ± 143	282 ± 148
Small-thin	349 ± 91	274 ± 39	244 ± 75
Large	249 ± 80	119 ± 24	115 ± 19

Values expressed as mean ± standard deviation.
*Indicates difference compared to wet Ag/AgCl ($p < 0.05$).

C. Cytotoxicity Test

The cytotoxicity of the electrodes was evaluated by placing the materials in direct contact with connective tissue cells (L929 cells) and primary human epidermal keratinocytes (NHEKs). Results were similar for each cell line. Microscopic analyses showed minimal cell death in monolayer cell cultures in contact with both autoclaved and antibiotic-sterilized electrodes (see Figs. 5 and 6). L929 cells cultured with electrodes [see Figs. 5(b) and (c)] remained adhered to the tissue culture plate and were morphologically consistent with cells cultured in the presence of the negative control material (HDPE) [see Fig. 5(a)] and without added material [see Fig. 5(e)]. Many of the cells appeared to be proliferating and confluence increased during the 24 h analysis period. Some cell death was observed immediately adjacent and under the electrode as well as the HDPE samples; however, the lack of a zone of inhibition extending beyond the margins of the sample suggests that this was due to cell death from compression and removal due to shear forces from sample micromotion associated with plate handling. In contrast, L929 monolayers cultured with latex positive controls were completely disrupted. The small number of L929 cells that remained were rounded and not well attached [see Fig. 5(d)]. Quantification of cellular viability using MTT solubilized with DMSO showed that metabolic activity of both cell types is not significantly altered by contact with electrodes compared to HDPE controls.

Cellular viability, as measured by average MTT reduction, of L929 cells cultured with HDPE was 31.0% lower than cell culture (no material) controls [see Fig. 5(f)]. The area of the HDPE sample occupies 30% of the growth area of a six well, suggesting that the loss of cell viability in these wells is primarily due to mechanical compression of the cells by the sample material. MTT reduction by L929 cells cultured with electrodes is not statistically different than by cells cultured with HDPE. MTT reduction by L929 cells cultured with latex is 84.4% lower than cell culture (no material) controls. These results suggest that the electrodes are not cytotoxic to L929 cells. Similarly, NHEK cells cultured in the presence of autoclaved or antibiotic-sterilized electrodes remained spread and maintained cell-cell contact [see Figs. 6(b) and (c)]. Morphologically, NHEK monolayers cultured with electrodes resembled monolayers cultured with HDPE negative controls [see Fig. 6(a)] and cell culture controls [see Fig. 6(e)]. NHEKs cultured with latex remained

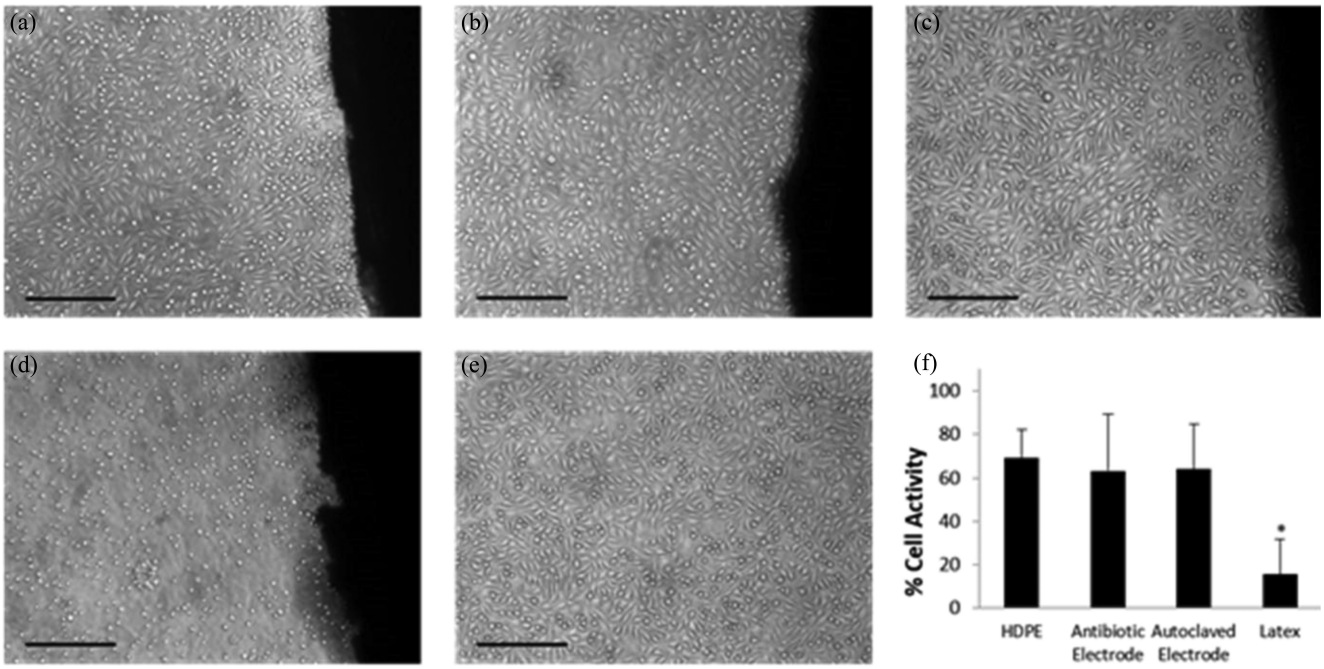

Fig. 5. Cytotoxic effect of electrodes on L929 cells. Phase contrast images of L929 cells after 24 h incubation with (a) HDPE, (b) antibiotic-sterilized electrode, (c) autoclaved electrode, (d) latex, or (e) no material. Material interface is visible at the right side of the images. Scale bars = 250 μm. (f) Cellular activity as determined by MTT assay (normalized to the no material control) is presented as mean + standard deviation. *Indicates statistical difference from all other materials ($p < 0.05$).

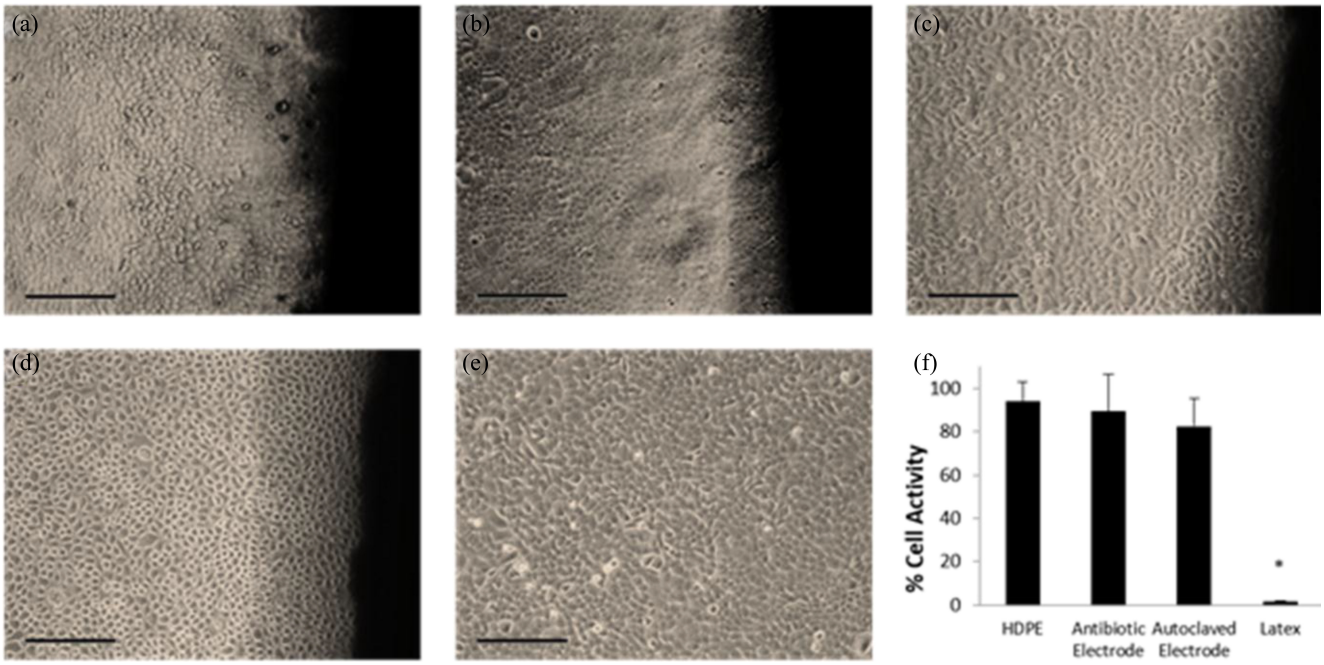

Fig. 6. Cytotoxic effect of electrodes on NHEK cells. Phase contrast images of NHEK cells after 24 h incubation with (a) HDPE, (b) antibiotic-sterilized electrode, (c) autoclaved electrode, (d) latex, or (e) no material. Material interface is visible at the right side of the images. Scale bars = 250 μm. (f) Cellular activity as determined by MTT assay (normalized to the no material control) is presented as mean + standard deviation. *Indicates statistical difference from all other materials ($p < 0.05$).

attached but exhibited rounded morphology and lacked cell-cell contact indicating cell death [see Fig. 6(d)]. Staining with MTT revealed that these cells were not metabolically active.

Since the electrodes are designed for skin contact, their cytotoxicity against NHEKs was also assessed [see Fig. 6(f)]. MTT reduction by NHEKs cultured with HDPE was 6.0% lower than by cells cultured with no material controls. There was no statistical difference between MTT reduction by NHEKs cultured with electrodes sterilized by either method and NHEKs cultured with HDPE. MTT reduction by cells cultured with

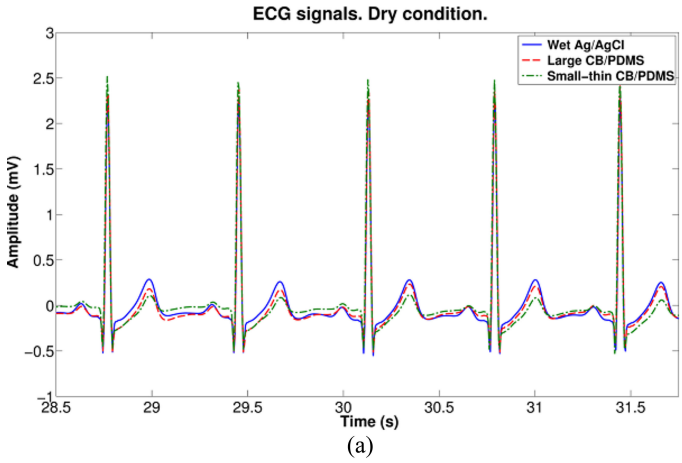

(a)

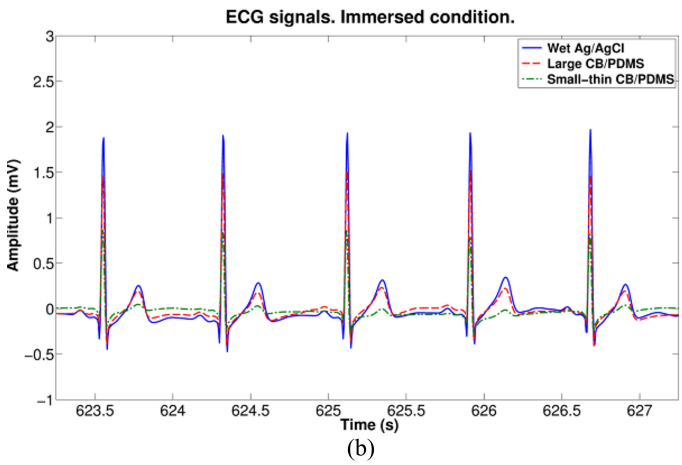

(b)

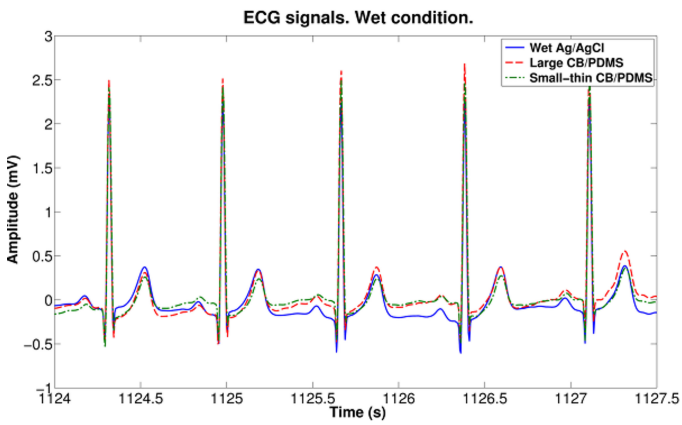

(c)

Fig. 7. Example of ECG signals for each experimental condition. (a) Initial outside period (dry condition). (b) Inside period (immersed condition). (c) Final outside period (wet condition). ECG signals acquired with wet Ag/AgCl electrodes (blue line), large CB/PDMS electrodes (red dashed line), and small-thin CB/PDMS electrodes (green dotted line).

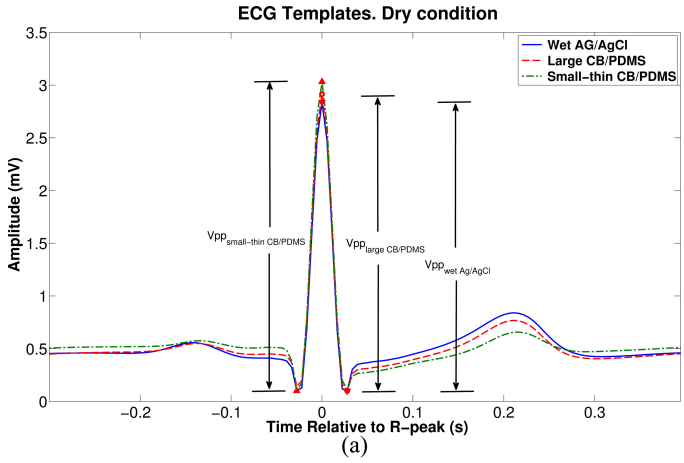

(a)

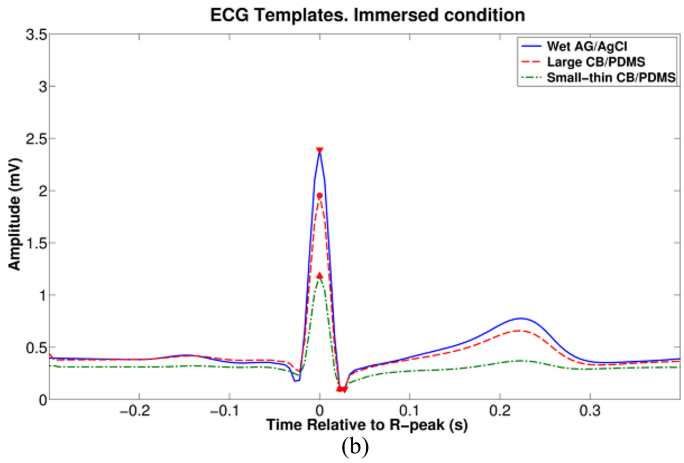

(b)

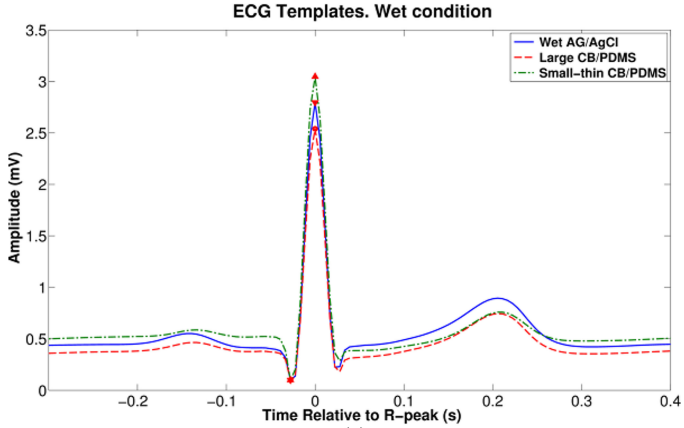

(c)

Fig. 8. Example of ECG templates for each experimental condition. (a) Initial outside period (dry condition). (b) Inside period (immersed condition). (c) Final outside period (wet condition). ECG signals acquired with wet Ag/AgCl electrodes (blue line), large CB/PDMS electrodes (red dashed line), and small-thin CB/PDMS electrodes (green dotted line).

latex was almost completely ablated (98.6%). These results demonstrate that the electrodes are not cytotoxic to NHEKs and in conjunction with the results on L929 cells suggest that the electrodes are not cytotoxic for epidermal applications.

D. ECG Signal Quality

1) Performance Evaluation of CB/PDMS Electrodes: ECG signals were simultaneously acquired with wet Ag/AgCl electrodes and large and small-thin CB/PDMS electrodes during three different conditions representing dry, full immersion, and postimmersion in which all electrodes were saturated with water but not fully immersed. The CB/PDMS electrodes were able

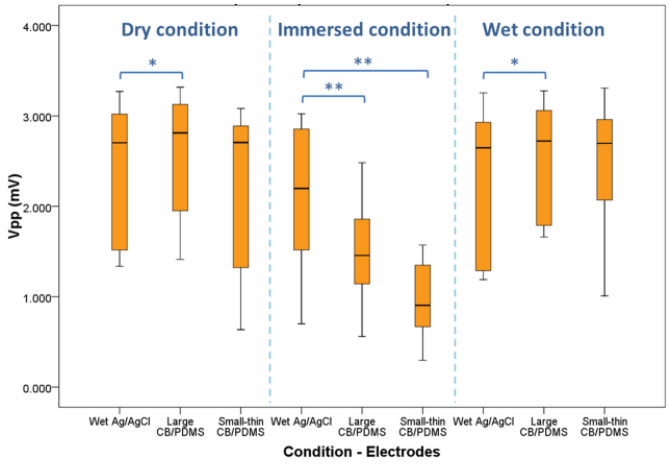

Fig. 9. Peak-to-peak amplitude of ECG templates for each condition. *indicates higher amplitudes versus Wet Ag/AgCl electrode ($p < 0.05$). *indicates lower amplitudes versus Wet Ag/AgCl electrode ($p < 0.05$).

to acquire ECG signals highly correlated with those from traditional wet Ag/AgCl electrodes during all conditions. Fig. 7 shows an example of filtered ECG signals recorded during each experimental condition with each type of CB/PDMS electrode as well as with wet Ag/AgCl. Fig. 8 shows an example of the ECG templates computed for each experimental condition with all tested electrodes. Both sizes of CB/PDMS electrodes were able to capture all morphological components of ECG signals during the dry, immersed, and wet conditions, and a decrease in amplitude especially for the small-thin CB/PDMS electrodes was only observed during the water immersed condition.

Statistical results of temporal and spectral HRV indices, peak-to-peak amplitudes, and cross-correlation coefficients obtained for the wet Ag/AgCl, large and small-thin CB/PDMS electrodes are summarized in Tables III, IV, and V, for the dry, immersed, and wet conditions, respectively. For all experimental conditions, no significant differences ($p > 0.05$) were found for all the temporal and spectral measures of HRV obtained with the CB/PDMS electrodes when compared to those obtained with the wet Ag/AgCl electrodes.

Waveform distortion of the ECG templates seems to be low as indicated by the high cross-correlation coefficient values for both CB/PDMS electrode sizes in comparison to the ECG templates obtained with wet Ag/AgCl electrodes during the dry, immersed, and wet conditions despite the amplitude differences.

Fig. 9 shows a boxplot with the results obtained for the peak-to-peak amplitude for each type of electrode during each experimental condition. The amplitude obtained with the large CB/PDMS electrode was found to be significantly higher compared to the wet Ag/AgCl amplitude ($p < 0.05$) during the dry condition. Both sizes of CB/PDMS electrodes produced lower amplitudes of ECG templates than the wet Ag/AgCl electrode during the immersed condition ($p < 0.05$). For the wet (postimmersion) condition, similar statistical results to the dry condition were obtained.

For the immersion and postimmersion conditions, amplitude attenuation/gain of ECG templates with respect to the initial preimmersion period was computed by dividing the peak-to-peak amplitude of the ECG template of the nondry conditions by the corresponding amplitude obtained during the dry condition with the same type of electrode. Table VI summarizes the amplitude attenuation/gain results for each type of electrode during immersion and postimmersion conditions relative to the dry condition. Amplitude reduction/gain results from CB/PDMS electrodes were compared to those from wet Ag/AgCl electrodes, and significantly lower reduction was found for both sizes of CB/PDMS when compared to the wet Ag/AgCl during the immersion condition ($p < 0.05$); for the wet condition, significantly higher gain was found for the small-thin CB/PDMS electrodes when compared to the wet Ag/AgCl ($p < 0.05$).

2) Without an Elastic Compression Band to Test True Hydrophobicity of Electrodes: To fully compare the hydrophobicity of the large carbon/PDMS and Ag/AgCl of electrodes, the elastic band was removed so that both sets of electrodes remained attached to the body only with their respective adhesive tapes [see Fig. 10(a), arrow]. The subjects were then fully immersed in a sitting position and were instructed to sit quietly [see Fig. 10(c)] for 1 min followed by moving their torso up-and-down [see Fig. 10(d)] and side-to-side [see Fig. 10(e)]. Fig. 11 shows representative recordings from two additional subjects. As shown in Figs. 10(c), the Ag/AgCl electrodes' ECG signals were immediately compromised even during a quiet sitting position, whereas for the CB/PDMS electrodes, high fidelity data can be seen. The Ag/AgCl electrodes' signal quality becomes saturated and consequently all morphological waveforms of the ECG are not discernible with both up-and-down and side-to-side movements as shown in Fig. 10(d), (e) and (a)–(d). Consequently, HR calculations cannot be performed. However, even with significant motion artifacts, the CB/PDMS electrodes are able to resolve QRS complexes throughout the data collection with body movements. There are visible low frequency oscillations which are due to cyclical body movements but they can be filtered to reveal all morphological waveforms of the ECG.

The average HR computed via an automatic R-peak detection algorithm is presented in Table VII for both types of electrodes for the ECG signal showed in Fig. 10. For the side-to-side torso movements, the mean HR value from the Ag/AgCl electrodes is about half the value of the CB/PDMS's. For the up-and-down torso movements, HR calculations cannot be determined for the Ag/AgCl electrodes since we obtain saturated values throughout the recording. For CB/PDMS electrodes, we obtain similar HR values as those at other conditions including the at rest period.

IV. Discussion

CB/PDMS electrodes of three different dimensions were fabricated (diameter × thickness: 2 cm × 2 mm, 2 cm × 3 mm, and 3 cm × 2 mm) as detailed in Section II. The SEM results indicated that the CB powders were fully dispersed inside the PDMS elastomeric matrix. Connectivity of CB/PDMS electrodes to conventional ECG and Holter monitors is made possible by using a snap connector attached to the electrodes during the fabrication process without compromising the structural integrity of the electrodes. The fabrication procedures can

TABLE III
ECG SIGNAL QUALITY INDICES—INITIAL PERIOD OUTSIDE WATER (DRY CONDITION)

	Parameter	Wet Ag/AgCl	CB/PDMS Large	CB/PDMS Small-thin
Temporal measures of HRV	meanNN(ms)	1384 ± 229	1384 ± 229	1384 ± 229
	SDNN (ms)	81 ± 20	82 ± 20	82 ± 20
	RMSSD (ms)	14 ± 4	14 ± 5	15 ± 4
	NN50 (unitless)	9 ± 12	10 ± 11	9 ± 11
Spectral measures of HRV	LF (ms^2)	3217 ± 1831	3222 ± 1838	3215 ± 1840
	HF (ms^2)	622 ± 539	638 ± 546	656 ± 529
	Total (ms^2)	6715 ± 2981	6766 ± 2971	6785 ± 2885
	LF/HF (unitless)	7.3 ± 4.2	7.3 ± 4.6	5.8 ± 3.0
Peak-to-peak amplitude	Vpp (mV)	2.39 ± 0.75	2.58 ± 0.69 *	2.19 ± 0.88
Cross-correlation index	ρ (unitless)	---	0.966 ± 0.051	0.923 ± 0.061

Values expressed as mean ± standard deviation.
*Indicates higher values compared to wet Ag/AgCl ($p < 0.05$).

TABLE IV
ECG SIGNAL QUALITY INDICES—PERIOD INSIDE WATER (IMMERSED CONDITION)

	Parameter	Wet Ag/AgCl	CB/PDMS Large	CB/PDMS Small-thin
Temporal measures of HRV	meanNN(ms)	1249 ± 214	1248 ± 213	1249 ± 214
	SDNN (ms)	71 ± 27	76 ± 24	73 ± 27
	RMSSD (ms)	16 ± 9	19 ± 9	18 ± 10
	NN50 (unitless)	8 ± 18	11 ± 19	10 ± 19
Spectral measures of HRV	LF (ms^2)	1232 ± 1120	1516 ± 1417	1232 ± 1113
	HF (ms^2)	789 ± 1422	1258 ± 1744	920 ± 1432
	Total (ms^2)	3885 ± 2884	4747 ± 3440	4114 ± 2988
	LF/HF (unitless)	2.9 ± 1.4	2.2 ± 1.2	2.4 ± 1.3
Peak-to-peak amplitude	Vpp (mV)	2.14 ± 0.79	1.52 ± 0.54 *	0.96 ± 0.43 *
Cross-correlation index	ρ (unitless)	---	0.978 ± 0.015	0.956 ± 0.029

Values expressed as mean ± standard deviation.
*Indicates lower values compared to wet Ag/AgCl ($p < 0.05$).

TABLE V
ECG SIGNAL QUALITY INDICES—FINAL PERIOD OUTSIDE WATER (WET CONDITION)

	Parameter	Wet Ag/AgCl	CB/PDMS Large	CB/PDMS Small-thin
Temporal measures of HRV	meanNN(ms)	1360 ± 266	1358 ± 265	1360 ± 266
	SDNN (ms)	98 ± 32	106 ± 34	99 ± 32
	RMSSD (ms)	16 ± 7	23 ± 16	17 ± 8
	NN50 (unitless)	16 ± 25	23 ± 29	17 ± 26
Spectral measures of HRV	LF (ms^2)	4062 ± 2611	4206 ± 2756	4076 ± 2622
	HF (ms^2)	1000 ± 1034	1778 ± 2591	1004 ± 1036
	Total (ms^2)	7765 ± 4181	9150 ± 6521	7780 ± 4186
	LF/HF (unitless)	9.2 ± 8.0	6.8 ± 7.5	9.2 ± 7.7
Peak-to-peak amplitude	Vpp (mV)	2.29 ± 0.80	2.54 ± 0.62 *	2.43 ± 0.74
Cross-correlation index	ρ (unitless)	---	0.983 ± 0.021	0.921 ± 0.067

Values expressed as mean ± standard deviation
*Indicates higher values compared to wet Ag/AgCl ($p < 0.05$)

TABLE VI
AMPLITUDE ATTENUATION OF ECG TEMPLATES WITH RESPECT TO SAME ELECTRODE DURING DRY CONDITION

Condition	Electrodes		
	Wet Ag/AgCl	Large CB/PDMS	Small-thin CB/PDMS
Dry	-	-	-
Immersed	0.878 ± 0.147	0.599 ± 0.185 *	0.449 ± 0.127 *
Wet	0.944 ± 0.059	0.997 ± 0.109	1.184 ± 0.262 *

Values expressed as mean ± standard deviation.
*Indicates difference compared to wet Ag/AgCl ($p < 0.05$).

be easily modified and optimized for large-scale production where the low cost of the carbon composite components will result in the CB/PDMS electrodes being fabricated economically. Certainly, the cost associated with the production of the CB/PDMS should be cheaper than Ag/AgCl since the cost of silver has significantly risen in the past few years. More importantly, while the Ag/AgCl electrodes are designed for a single use, our CB/PDMS electrodes may be reused hence resulting in significant cost savings. Furthermore, unlike Ag/AgCl electrodes, our CB/PDMS electrodes do not have a finite shelf life. It is well known that even when Ag/AgCl electrodes are contained in a sealed package, if they are not used within a certain

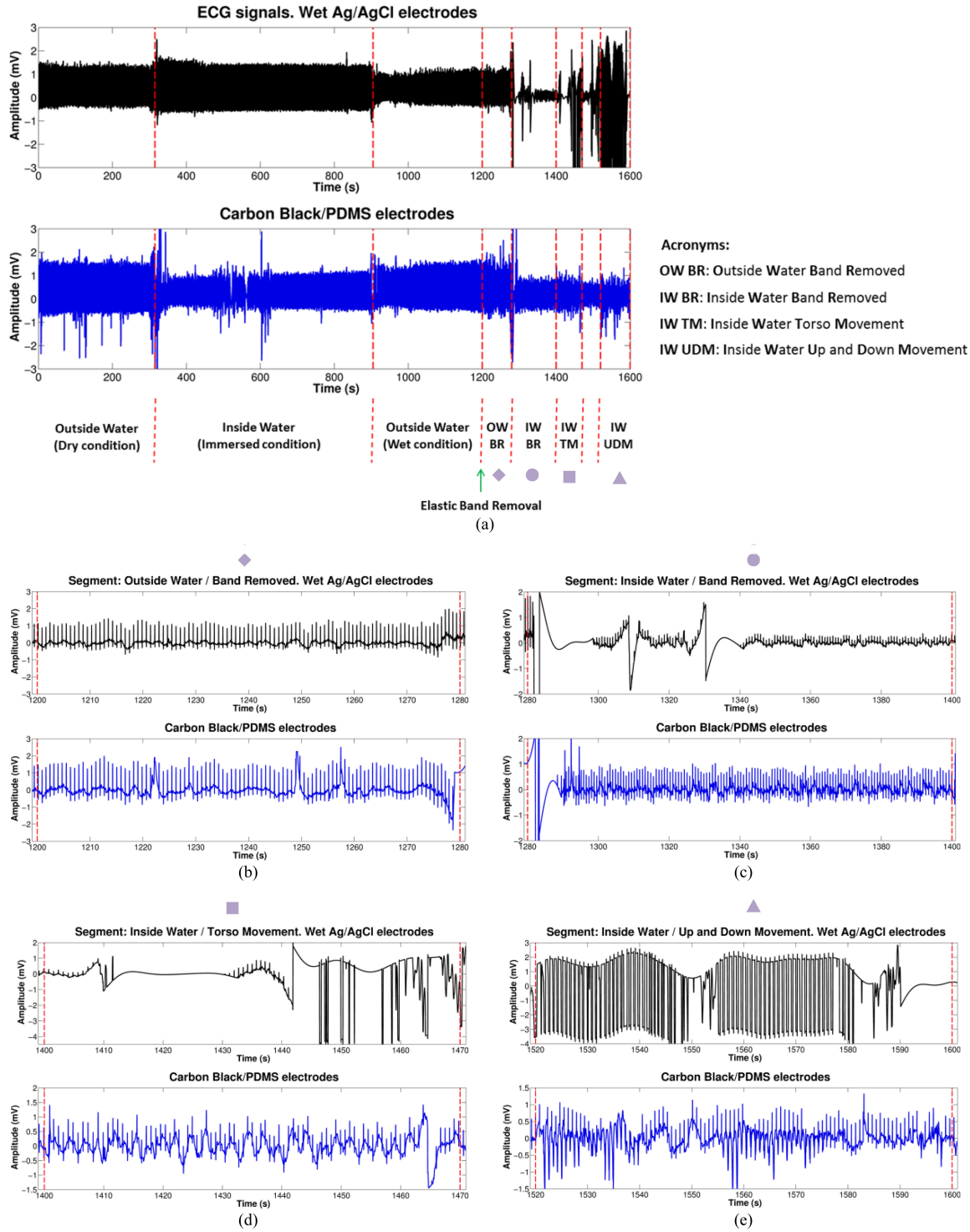

Fig. 10. ECG recording on surface and underwater with wet Ag/AgCl and CB/PDMS electrodes during different conditions. (a) Full recording with aligned and filtered ECG signals. Dry condition: subject outside water, standing. Immersed condition: subject inside water, seated. Wet condition: subject outside water, standing. (b) OW-BR segment: subject outside water without elastic band, standing. (c) IW-BR segment: subject inside water without elastic band, seated. (d) IW-DM segment: torso movement inside water without elastic band, seated. (e) IW-UDM: up and down movement inside water without elastic band, seated. Dry, immersed, and wet conditions were further explored in this letter.

time limit (usually 1 year), the hydrogels dry out resulting in low-fidelity ECG signals.

Impedance of skin-CB/PDMS electrodes was investigated as a function of electrode dimensions. Impedance values of the CB/PDMS electrodes varied according to their sizes with the largest electrodes (3 cm $\times$ 2 mm) having the lowest impedance, which is in accordance with the classical resistance law in terms of the material resistivity and electrode dimensions [29]. Influence of the pressure level applied to the electrode against the recording site was also studied and was found to be

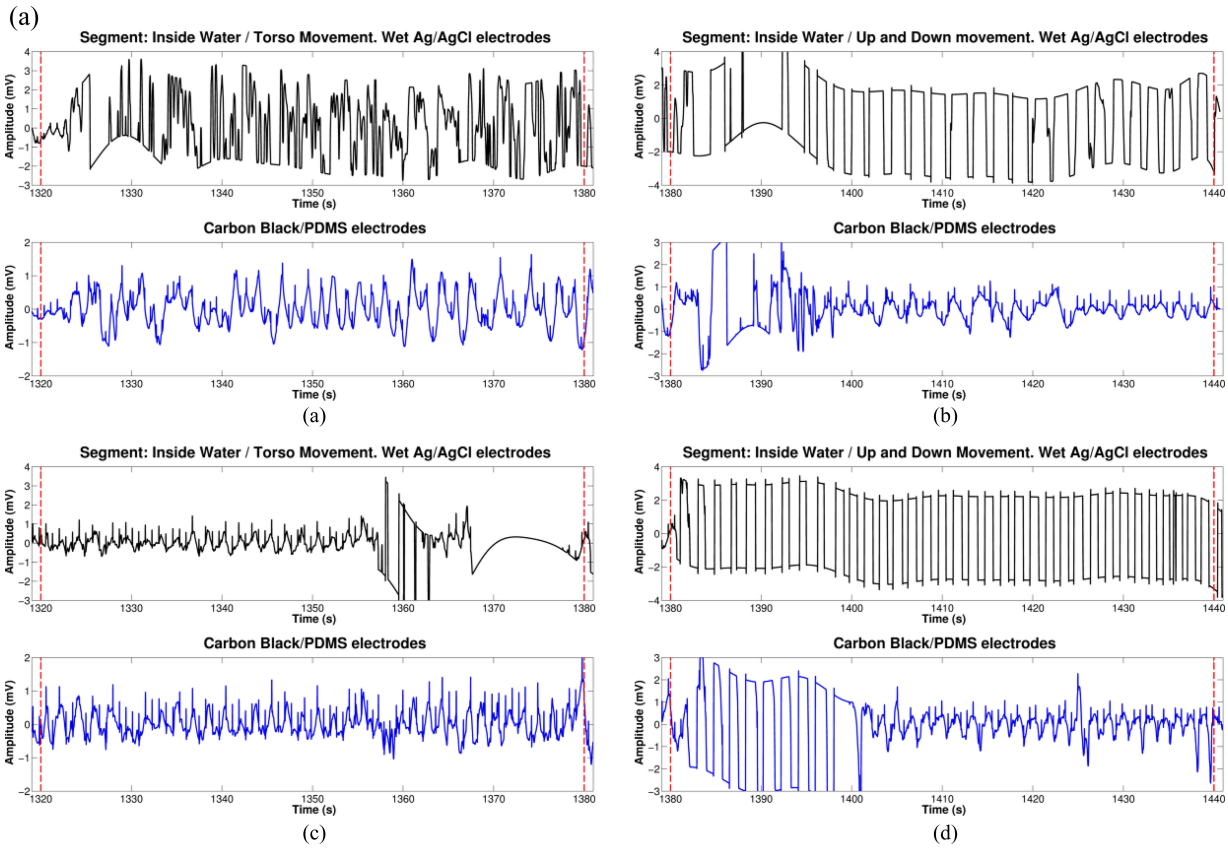

Fig. 11. Examples of ECG recordings underwater with wet Ag/AgCl and CB/PDMS electrodes during movement conditions. (a) and (c) Torso movement inside water without elastic band, seated. (b) and (d) Up and down movement inside water without elastic band, seated.

TABLE VII
AVERAGE HR COMPARED FOR THE DIFFERENT CONDITIONS OF THE RECORDING SHOWN IN FIG. 10

Condition	Wet Ag/AgCl electrodes Average Heart Rate (bpm)	CB/PDMS electrodes Average Heart Rate (bpm)
Dry	76.6	77.2
Immersed	71.7	71.2
Wet	79.6	78.4
Outside Water / Band Removed	76.3	75.6
Inside Water / Band Removed	63.9	76.5
Torso Movement / Band Removed	37.0	75.8
Up & Down Movement / Band Removed	- -	75.3

dependent on the applied pressure, in agreement with a previous study [16]. For the same electrode size, skin-electrode impedance decreased as the pressure level increased. It was found that for thinner CB/PDMS electrodes the decrement in skin-CB/PDMS electrode impedance was markedly less for a medium and a high pressure level when compared to thicker electrodes. This could be explained by taking into account the elastic properties of PDMS elastomer and the conductive network formation through PDMS by the CB contents. As the CB concentration increases when the electrode is compressed against the skin, the distance between particles decreases and facilitates the transport of electrons through connected particles by a tunneling effect [20], [30], [31]. However, as seen in Figs. 4(b) and (c), the impedance values do not significantly decrease even when higher-than-medium pressure is applied since after a certain pressure threshold, CB conductive elements do not compress further and, hence, no further conductive pathways are formed. Since lower impedance leads to better signal conduction in dry condition, the large and small-thin CB/PDMS electrodes were selected for underwater ECG testing.

Cytotoxicity of CB/PDMS electrodes was evaluated with connective tissue cells and primary human epidermal keratinocytes. Similar results were found for each cell line and demonstrate that the electrodes are not cytotoxic for epidermal applications. Although motion artifacts were not fully explored in this paper, we expect that due to their flexibility, CB/PDMS electrodes adapt better to skin topography than rigid dry electrodes which are prone to shifting against skin during body movement [16].

While there have been other carbon-based ECG electrode developments [14], we are not aware of their capacity to function in full water immersion. The use of PDMS polymers is popular due to their simple and inexpensive fabrication process, but

the most attractive features are the superior elasticity and flexibility, nontoxicity to cells, high-permeability to oxygen, and impermeability to water [22], [32], [33]. Obtaining conductive materials with low resistivity by introducing CB in a polymer matrix has been previously performed [34]. However, in contrast to carbon nanotubes where the homogenous dispersal in thick PDMS is challenging, CB particles have been found to be easy to mix with PDMS gel and they distribute uniformly [35]. The conductivity of CB/PDMS composites has been found to increase rapidly beyond a threshold concentration (circa 10 wt%) [36]. While these studies have characterized basic properties of combining PDMS and carbon powder, fabrication of electrodes for application to ECG recordings has not been done.

To this end, we tested the CB/PDMS electrodes during full immersion followed by post-immersion and compared their performance against the wet (i.e., gel-filled) Ag/AgCl electrodes. It is well known that water is a good electric conductor with respect to skin-electrode impedance, but it acts as a short-circuit for poorly insulated electrodes, hence recording of biopotentials requires sufficient electrical insulation [12], [15]. Our results show that the morphologies of the ECG waveforms obtained were comparable to that of the wet Ag/AgCl electrodes and that all ECG morphologies were captured even during full water immersion.

Quantification of the fidelity of the CB/PDMS electrodes was achieved by using HRV analysis for dry and water immersion and post-water immersion conditions. Note that during these procedures, a nonwaterproof elastic compression band was wrapped over all electrodes to ensure that electrodes adhered tightly to the skin. While the R-wave amplitude was significantly reduced during immersion when compared to the dry conditions, the reduction was small. Hence, Ag/AgCl electrodes benefited from water not fully penetrating the hydrogels, allowing us to record good ECG signals even during full water immersion. The reason for using an elastic compression band was to obtain nonwater contaminated ECG signals from the Ag/AgCl electrodes so that we can make direct comparison to the CB/PDMS electrodes. For all conditions, we found nonsignificant differences in both time- and frequency-domain parameters for both sizes of CB/PDMS electrodes when compared to the wet Ag/AgCl electrodes. During the initial surface period, i.e., dry condition, ECG amplitudes obtained with large CB/PDMS electrodes were significant higher than those from the wet Ag/AgCl electrodes. The same results were obtained during the postimmersion period. We surmise that the increase of ECG amplitudes seen during post-water immersion with CB/PDMS electrodes can be attributed to the fact that some remnant water on the electrodes facilitated better electrical signal conduction than dry condition. Note that water is a good conductor, hence, its impedance is lower than skin. Therefore, when CB/PDMS electrodes are fully water immersed, electrical biopotentials will follow the path of least resistance and especially for those currents near the edges of the electrode will flow through water rather than skin. We believe this is why reduction in the amplitudes of the ECG R-wave peak is observed during immersion. As salt water is an even better conductor (the resistance may drop to as low as $10\,\Omega$) than non-salt water, we expect further degradation of R-wave amplitudes with the CB/PDMS during immersion in ocean water. In our study, we also noted significant R-wave amplitude reduction during immersion and postimmersion when compared to the dry condition for the Ag/AgCl electrodes. This is also expected since the typical Ag/AgCl electrode-skin-electrode impedance is on the order of kilo ohms as shown in Fig. 4, whereas water electrode-skin-electrode impedance is on the order of several hundred ohms. On average, there was a reduction of 40% for the large CB/PDMS electrodes and 65% for the small-thin CB/PDMS, and 12% for the Ag/AgCl electrodes.

For the next set of experiments, we removed the elastic compression band and recorded ECG signals from both CB/PDMS and Ag/AgCl electrodes. The goal was to examine how these electrodes perform after being exposed to more than 30 min of water immersion and with body movements but without the elastic compression band. No new tape was applied to the CB/PDMS electrodes or to the Ag/AgCl electrodes. As shown in Figs. 10 and 11, we observe that when water penetrates the Ag/AgCl electrodes due to body movements, we often observe saturated ECG signals resulting in nondiscernible ECG waveform morphologies. For the CB/PDMS electrodes, while they are affected by the low-frequency body movements, all morphological waveforms were discernible. Clearly, this is the key desired feature of our CB/PDMS electrodes.

Other applications of CB/PDMS electrodes may include EEG and electromyogram (EMG) studies. In particular, underwater EMG recording is widely used for research, exercise training, and rehabilitation treatments using swimming pools [37], [38].

V. Conclusion

The CB/PDMS electrodes were fabricated and tested in both dry and water immersion conditions. All morphological ECG waveforms were acquired with the CB/PDMS electrodes for both conditions albeit the R-wave amplitude was significantly reduced when the electrodes including Ag/AgCl were exposed to water. Body movements during water immersion caused water penetration to Ag/AgCl electrodes and, consequently, no discernible ECG waveforms were seen. However, for the CB/PDMS electrodes, despite full water exposure and severe body movements, all morphological waveforms of ECG signals were resolved. For nonwater immersed conditions, we found no statistical difference in the HRV time- and frequency-domain parameters when compared to Ag/AgCl electrodes.

The use of CB/PDMS electrodes together with advanced waterproof diving instruments may open up new research areas including hyperbaric physiology and may lead to wide use as vital sign monitoring devices for SCUBA divers. Early detection of conditions that could lead to decompression sickness is another area where an ECG dive monitor could have a positive impact on recreational and military SCUBA divers.

References

[1] C. W. Mundt, K. N. Montgomery, U. E. Udoh, V. N. Barker, G. C. Thonier, A. M. Tellier, R. D. Ricks, B. B. Darling, Y. D. Cagle, N. A. Cabrol, S. J. Ruoss, J. L. Swain, J. W. Hines, and G. T. A. Kovacs, "A multiparameter wearable physiologic monitoring system for space and

terrestrial applications," *IEEE Trans. Inf. Technol. Biomed.*, vol. 9, no. 3, pp. 382–391, Sep. 2005.
[2] G. Bosco, G. D. Tano, V. Zanon, and G. Fanò, "Breath-hold diving: A point of view," *Sport Sci. Health*, vol. 2, no. 2, pp. 47–54, Dec. 2007.
[3] J. Hansel, I. Solleder, W. Gfroerer, C. M. Muth, K. Paulat, P. Simon, H. C. Heitkamp, A. Niess, and K. Tetzlaff, "Hypoxia and cardiac arrhythmias in breath-hold divers during voluntary immersed breath-holds," *Eur. J. Appl. Physiol.*, vol. 105, no. 5, pp. 673–678, Mar. 2009.
[4] K. Hirayanagi, K. Nakabayashi, K. Okonogi, and H. Ohiwa, "Autonomic nervous activity and stress hormones induced by hyperbaric saturation diving," *Undersea Hyperb. Med.*, vol. 30, no. 1, pp. 46–54, 2003.
[5] A. Kurita, H. Nagayoshi, Y. Okamoto, B. Takase, T. Ishizuka, and H. Oiwa, "Effects of severe hyperbaric pressure on autonomic nerve functions," *Mil. Med.*, vol. 167, no. 11, pp. 934–938, Nov. 2002.
[6] Y. Bai, R. T. Mahon, J. C. White, P. R. Brink, and K. H. Chon, "Impairment of the autonomic nervous function during decompression sickness in swine," *J. Appl. Physiol.*, vol. 106, no. 3, pp. 1004–1009, Mar. 2009.
[7] J. P. Florian, "Repeated 6-h oxygen dives diminish dynamic and static exercise performance," *Undersea Hyperb Med*, vol. 37, p. 335, 2010.
[8] "Heart rate variability. standards of measurement, physiological interpretation, and clinical use. task force of the european society of cardiology and the North American society of pacing and electrophysiology," *Eur. Heart J.*, vol. 17, no. 3, pp. 354–381, Mar. 1996.
[9] P. Lindholm and C. E. Lundgren, "The physiology and pathophysiology of human breath-hold diving," *J. Appl. Physiol.*, vol. 106, no. 1, pp. 284–292, Jan. 2009.
[10] Y. Bai, N. Selvaraj, K. Petersen, R. Mahon, W. A. Cronin, J. White, P. R. Brink, and K. H. Chon, "The autonomic effects of cardiopulmonary decompression sickness in swine using principal dynamic mode analysis," *Amer. J. Physiol. Regul. Integr. Comp. Physiol.*, vol. 305, no. 7, pp. R748–758, Oct. 2013.
[11] W. I. Sternberger and S. A. Goemmer, "Advanced dive monitoring system," *Life Support Biosphere Sci. Int. J. Earth Space*, vol. 6, no. 3, pp. 251–258, 1999.
[12] A. Sieber, A. L'Abbate, B. Kuch, M. Wagner, A. Benassi, M. Passera, and R. Bedini, "Advanced instrumentation for research in diving and hyperbaric medicine," *Undersea Hyperb Med.*, vol. 37, pp. 259–269, 2010.
[13] Y. M. Chi, T. P. Jung, and G. Cauwenberghs, "Dry-contact and noncontact biopotential electrodes: Methodological review," *Biomed. Eng. IEEE Rev.*, vol. 3, no. 1, pp. 106–119, Oct. 2010.
[14] H. C. Jung, J. H. Moon, D. H. Baek, J. H. Lee, Y. Y. Choi, J. S. Hong, and S. H. Lee, "CNT/PDMS composite flexible dry electrodes for long-term ECG monitoring," *IEEE Trans. Biomed. Eng.*, vol. 59, no. 5, pp. 1472–1479, May 2012.
[15] P. F. Hoar, H. C. Langworthy, W. H. Mints, W. E. Long, and L. W. Raymond, "Technique for electrocardiographic monitoring of working divers," *Aviat. Space Environ. Med.*, vol. 47, no. 6, pp. 667–671, Jun. 1976.
[16] A. Gruetzmann, S. Hansen, and J. Müller, "Novel dry electrodes for ECG monitoring," *Physiol. Meas.*, vol. 28, no. 11, p. 1375, Nov. 2007.
[17] J. Y. Baek, J. H. An, J. M. Choi, K. S. Park, and S. H. Lee, "Flexible polymeric dry electrodes for the long-term monitoring of ECG," *Sens. Actuators Phys.*, vol. 143, no. 2, pp. 423–429, May 2008.
[18] G. Ruffini, S. Dunne, L. Fuentemilla, C. Grau, E. Farrés, J. Marco-Pallarés, P. C. P. Watts, and S. R. P. Silva, "First human trials of a dry electrophysiology sensor using a carbon nanotube array interface," *Sens. Actuators Phys.*, vol. 144, no. 2, pp. 275–279, Jun. 2008.
[19] L. F. Wang, J. Q. Liu, B. Yang, and C. S. Yang, "PDMS-based low cost flexible dry electrode for long-term EEG measurement," *IEEE Sens. J.*, vol. 12, no. 9, pp. 2898–2904, Sep. 2012.
[20] M. L. Homer, J. R. Lim, K. Manatt, A. Kisor, A. M. Manfreda, L. Lara, A. D. Jewell, S. P. S. Yen, H. Zhou, A. V. Shevade, and M. A. Ryan, "Temperature effects on polymer-carbon composite sensors: evaluating the role of polymer molecular weight and carbon loading," in *Proc. IEEE Sensors*, 2003, vol. 2, pp. 877–881.
[21] M. Leboeuf, N. Ghamri, B. Brulé, T. Coupez, and B. Vergnes, "Influence of mixing conditions on rheological behavior and electrical conductivity of polyamides filled with carbon black," *Rheol. Acta*, vol. 47, no. 2, pp. 201–212, Mar. 2008.
[22] H. Cong and T. Pan, "Photopatternable conductive PDMS materials for microfabrication," *Adv. Funct. Mater.*, vol. 18, no. 13, pp. 1912–1921, 2008.
[23] M. K. Delano and C. G. Sodini, "A long-term wearable electrocardiogram measurement system," in *Proc. IEEE Int. Conf. Body Sensor Netw.*, 2013, pp. 1–6.
[24] B. H. Tracey and E. L. Miller, "Nonlocal means denoising of ECG signals," *IEEE Trans. Biomed. Eng.*, vol. 59, no. 9, pp. 2383–2386, Sep. 2012.
[25] A. Buades, B. Coll, and J. M. Morel, "A review of image denoising algorithms, with a new one," *Simul*, vol. 4, pp. 490–530, 2005.
[26] V. X. Afonso, W. J. Tompkins, T. Q. Nguyen, and S. Luo, "ECG beat detection using filter banks," *IEEE Trans. Biomed. Eng.*, vol. 46, no. 2, pp. 192–202, Feb. 1999.
[27] C. Vidaurre, T. H. Sander, and A. Schlögl, "BioSig: The free and open source software library for biomedical signal processing," *Comput. Intell. Neurosci.*, vol. 2011, pp. 1–12, Mar. 2011.
[28] A. D. Flouris and J. M. Scott, "Heart rate variability responses to a psychologically challenging scuba dive," *J. Sports Med. Phys. Fitness*, vol. 49, no. 4, pp. 382–386, Dec. 2009.
[29] J. G. Webster, *Medical Instrumentation: Application and Design*. New York, NY, USA: Wiley, 1998.
[30] S. Kohjiya, A. Katoh, J. Shimanuki, T. Hasegawa, and Y. Ikeda, "Nanostructural observation of carbon black dispersion in natural rubber matrix by three-dimensional transmission electron microscopy," *J. Mater. Sci.*, vol. 40, no. 9–10, pp. 2553–2555, May 2005.
[31] S. P. Rwei, F. H. Ku, and K. C. Cheng, "Dispersion of carbon black in a continuous phase: Electrical, rheological, and morphological studies," *Colloid Polym. Sci.*, vol. 280, no. 12, pp. 1110–1115, Dec. 2002.
[32] S. K. Sia and G. M. Whitesides, "Microfluidic devices fabricated in Poly(dimethylsiloxane) for biological studies," *Electrophoresis*, vol. 24, no. 21, pp. 3563–3576, 2003.
[33] J. Zhou, A. V. Ellis, and N. H. Voelcker, "Recent developments in PDMS surface modification for microfluidic devices," *Electrophoresis*, vol. 31, no. 1, pp. 2–16, 2010.
[34] E. K. Sichel *Carbon Black-Polymer Composites: The Physics Of Electrically Conducting Composites*. M. Dekker Ed., Adelaide, Australia Science 1982.
[35] X. Z. Niu, S. L. Peng, L. Y. Liu, W. J. Wen, and P. Sheng, "Characterizing and patterning of PDMS-based conducting composites," *Adv. Mater.*, vol. 19, no. 18, pp. 2682–2686, 2007.
[36] M. A. Unger, H. P. Chou, T. Thorsen, A. Scherer, and S. R. Quake, "Monolithic microfabricated valves and pumps by multilayer soft lithography," *Science*, vol. 288, no. 5463, pp. 113–116, Apr. 2000.
[37] A. Rainoldi, C. Cescon, A. Bottin, R. Casale, and I. Caruso, "Surface EMG alterations induced by underwater recording," *J. Electromyogr. Kinesiol.*, vol. 14, no. 3, pp. 325–331, Jun. 2004.
[38] W. M. Silvers and D. G. Dolny, "Comparison and reproducibility of sEMG during manual muscle testing on land and in water," *J. Electromyogr. Kinesiol.*, vol. 21, no. 1, pp. 95–101, Feb. 2011.

Authors' photographs and biographies not available at the time of publication.